Glass transition in soft-sphere dispersions

2009 J. Phys.: Condens. Matter 21 075101

(http://iopscience.iop.org/0953-8984/21/7/075101)

J. Phys.: Condens. Matter **21** (2009) 075101 (13pp) doi:10.1088/0953-8984/21/7/075101

Glass transition in soft-sphere dispersions

P E Ramírez-González and M Medina-Noyola

Instituto de Física 'Manuel Sandoval Vallarta', Universidad Autónoma de San Luis Potosí, Álvaro Obregón 64, 78000 San Luis Potosí, SLP, Mexico

Received 14 July 2008, in final form 3 November 2008
Published 5 January 2009
Online at stacks.iop.org/JPhysCM/21/075101

Abstract

The concept of dynamic equivalence among mono-disperse soft-sphere fluids is employed in the framework of the self-consistent generalized Langevin equation (SCGLE) theory of colloid dynamics to calculate the ideal glass transition phase diagram of model soft-sphere colloidal dispersions in the softness–concentration state space. The slow dynamics predicted by this theory near the glass transition is compared with available experimental data for the decay of the intermediate scattering function of colloidal dispersions of soft-microgel particles. Increasing deviations from this simple scheme occur for increasingly softer potentials, and this is studied here using the Rogers–Young static structure factor of the soft-sphere systems as the input of the SCGLE theory, without assuming *a priori* the validity of the equivalence principle above.

(Some figures in this article are in colour only in the electronic version)

1. Introduction

One of the most useful models in the statistical physics of liquids is the hard-sphere fluid. Although this is a mathematical idealization, its properties serve as a first-order approximation for those of real simple liquids [1], including 'simple' colloidal dispersions, in which the colloidal particles play the role of the atoms in atomic systems [2, 3]. For example, the thermodynamic and structural properties of systems of particles interacting through *soft* repulsive interactions may be shown to map onto the properties of an equivalent hard-sphere fluid at the same number concentration but with an effective hard-sphere diameter determined by simple physical considerations, such as those leading to the 'blip function' method of Andersen, *et al* [1, 4]. In fact, this mapping allows us to approximate the properties of real simple liquids, adequately modeled by a steep but soft repulsion plus an additional attractive term, as in the Lennard-Jones potential, by the sum of the properties of an effective hard-sphere reference system plus a smaller perturbation representing the contribution of the attractive interactions [1, 4].

This structural equivalence between soft-sphere and hard-sphere systems has been employed to describe not only the thermodynamic and structural properties of soft-sphere systems, but also their dynamic properties [5]. It is, however, not an exact result, and the accuracy of its predictions depends on the specific property studied [6]; thus, for each such property one should identify the softness regime where this structural scaling is a useful approximation and the regime where it is not. In the regime where it is shown to hold, however, not only must the topology of the equilibrium phase diagram of soft-sphere systems be trivially equivalent to that of the hard-sphere model, but also the existence and location of the dynamic arrest transition [7–9] in these systems could be inferred from the existence and location of the corresponding glass transition in the hard-sphere model. Thus, the description of the dynamic properties of colloidal dispersions of particles interacting through some form of soft-core potentials (microgel colloids [10], star polymers with a large number of arms [11], etc) would be rather straightforward, in the sense that they could be obtained from the corresponding properties of the hard-sphere system by simple rescaling arguments. This equivalence must apply more accurately for soft but very steep potentials, and must break down for extremely soft interactions. In fact, it has been found that simple mono-disperse systems involving ultra-soft repulsive interactions may exhibit qualitatively new features [12], not observed in the hard-sphere system. It is then important to investigate the range of validity of this equivalence in the context of particular families of soft repulsive potentials and of specific kinds of physical properties of these models.

With the aim of better understanding available experimental information on the glassy dynamics of soft-sphere dispersions [10], in this work we address this question in the context of the dynamic properties of dispersions of soft colloidal particles. We are interested in particular in the slow dynamics of these systems near their glass transition, and more specifically, in the location of the glass transition line in the softness–concentration state space. For this, we consider one specific family of repulsive soft-sphere interactions, namely, the trun-

cated Lennard-Jones-like potential given, in units of the thermal energy $k_B T = \beta^{-1}$, by

$$\beta u^{(\nu)}(r) = \epsilon^* \left[\frac{1}{(r/\sigma)^{2\nu}} - \frac{2}{(r/\sigma)^{\nu}} + 1 \right], \qquad (1.1)$$

for $0 < r < \sigma$, and such that it vanishes for $r > \sigma$. The positive parameter ν determines the degree of softness of this pair potential, and the limit $\nu \to \infty$ corresponds to the hard-sphere system. The dimensionless energy scale ϵ^* could also be used to modulate the effective degree of softness, but in order to simplify our discussion we shall keep this parameter fixed to $\epsilon^* = 1$. Between collisions, the dispersed particles are assumed to execute Brownian motion, characterized by a diffusion coefficient D_0. In systems with strong hydrodynamic interactions we shall assume that D_0 can be identified with the short-time self-diffusion coefficient [2, 13].

We shall base our description of the macroscopic dynamic properties of this system on the self-consistent generalized Langevin equation (SCGLE) theory of colloid dynamics [14, 15], and more specifically on the predictions of this theory regarding the dynamic arrest transitions in mono-disperse suspensions [16–18]. The SCGLE theory was originally devised to describe the tracer and collective diffusion properties of colloidal dispersions in the short- and intermediate-time regimes. Its self-consistent character, however, introduces a non-linear dynamic feedback, leading to the prediction of dynamic arrest, similar to that exhibited by the mode coupling theory (MCT) of the ideal glass transition [9]. The application of this theory was first illustrated with the comparison of its predictions of the glass transition in two mono-disperse experimental systems with specific (hard-sphere and screened electrostatic) interparticle effective forces [17]. For these systems the SCGLE theory was found to have similar quantitative predictive power as conventional MCT, but with a lower degree of difficulty in its application [18]. Some aspects of the application of the SCGLE theory to systems with short-ranged attractive interactions were also reported in recent communications [16, 19].

In the following section we review the basic elements of the SCGLE theory of dynamic arrest. This theory requires the static structure factor $S(k)$ of the system as an external input. Here we resort to two strategies to calculate $S(k)$. The first consists of the simplest analytic approximation for $S(k)$, based precisely on the assumed static equivalence between soft- and hard-sphere systems, for which the Percus–Yevick approximation [20, 21], complemented with the Verlet–Weiss correction [22], provides virtually exact analytic results; in the appendix we summarize the details of this simple approximate scheme to determine $S(k)$. The second strategy is based on the numerical solution of the Ornstein–Zernike equation within the Rogers–Young approximation [23], without resorting to the equivalence principle above.

The dynamic extension of the static equivalence principle between soft- and hard-sphere systems is discussed within the framework of the SCGLE theory in section 3 and in the appendix. This extension leads to simple scaling rules that allow us to approximate the dynamic properties of soft-sphere systems by those of the hard-sphere system, easily described by the SCGLE theory [17, 18]; thus, we solve the full self-consistent system of equations of the SCGLE theory for the hard-sphere system to determine the time and wavevector dependence of the collective dynamic properties of any other moderately soft-sphere system. The predictive power of this extremely simple scheme is then tested in section 4, by comparing its predictions with available experimental data of the dynamics of a specific soft-sphere system near its glass transition. The comparison of these calculations with the experimental results is found to be reasonably accurate not only qualitatively but also quantitatively.

Since this simple theoretical scheme must eventually break down for soft enough interactions, i.e. for low enough values of ν, in section 5 we discuss the deviations from this hard-sphere-like behavior of soft-sphere systems. For this we resort to the second, more accurate, strategy to calculate the static structure factor involving the Rogers–Young approximation [23]. The comparison of the resulting phase diagram with that determined in section 3 on the basis of the equivalence principle provides an indication of the limits of validity of the simple scheme of section 3. The main conclusions of this paper are finally summarized in section 4.

2. Brief review of the SCGLE theory

The dynamic properties of colloidal dispersions can be described in terms of the relaxation of the fluctuations $\delta n(\mathbf{r}, t)$ of the local concentration $n(\mathbf{r}, t)$ of colloidal particles around its bulk equilibrium value n. The average decay of $\delta n(\mathbf{r}, t)$ is described by the time-dependent correlation function $F(k, t) \equiv \langle \delta n(\mathbf{k}, t) \delta n(-\mathbf{k}, 0) \rangle$ of the Fourier transform $\delta n(\mathbf{k}, t) \equiv (1/N) \sum_{i=1}^{N} \exp[i\mathbf{k} \cdot \mathbf{r}_i(t)]$ of the fluctuations $\delta n(\mathbf{r}, t)$, with $\mathbf{r}_i(t)$ being the position of particle i at time t. $F(k, t)$ is referred to as the intermediate scattering function. One can also define the self-component of $F(k, t)$, referred to as the self-intermediate scattering function, as $F_S(k, t) \equiv \langle \exp[i\mathbf{k} \cdot \Delta\mathbf{R}(t)] \rangle$, where $\Delta\mathbf{R}(t)$ is the displacement of any of the N particles over a time t. The self-consistent generalized Langevin equation theory of colloid dynamics [14, 15] leads to the calculation of $F(k, t)$ and $F_S(k, t)$, given the effective interaction pair potential $u(r)$ between colloidal particles and the corresponding equilibrium static structure, represented by the static structure factor $S(k)$.

This theory is based on general and exact expressions for $F(k, t)$ and $F_S(k, t)$ in terms of a hierarchy of memory functions complemented by a number of physically or intuitively motivated approximations [14]. The first and most important of such elements consists of general and exact memory-function expressions for $F(k, t)$ and $F_S(k, t)$, which, in Laplace space, read [14]

$$F(k, z) = \frac{S(k)}{z + \frac{k^2 D_0 S^{-1}(k)}{1 + C(k, z)}}, \qquad (2.1)$$

$$F_S(k, z) = \frac{1}{z + \frac{k^2 D_0}{1 + C_S(k, z)}}, \qquad (2.2)$$

where D_0 is the diffusion coefficient describing the particles' motion between collisions, $S(k)$ is the static structure factor of the system, and $C(k,z)$ and $C_S(k,z)$ are the Laplace transform (LT) of the so-called irreducible memory functions $C(k,t)$ and $C_S(k,t)$ [24][1]. These exact results can be derived in a variety of manners, and our derivation was framed within the generalized Langevin equation (GLE) formalism and the process of contraction of the description [26, 27].

The second ingredient of the SCGLE theory is the intuitive notion that collective and self-dynamics may be connected in a simple manner. Vineyard's approximation [28], in which the collective propagator $\Psi(k,t) \equiv F(k,t)/S(k)$ is approximated by the 'self'-propagator $\Psi^{(s)}(k,t) \equiv F^{(s)}(k,t)$, is the most primitive (or 'zeroth-order') implementation of this idea. Equations (2.1) and (2.2) suggest, however, that other connections between self- and collective dynamics may be proposed at the level of the memory functions $C(k,z)$ and $C_S(k,z)$, the simplest of them being to approximate one by the other, namely,

$$C(k,t) = C_S(k,t). \tag{2.3}$$

This is referred to as the first-order Vineyard approximation, and is the approximation that we shall incorporate in the SCGLE theory of dynamic arrest employed in the present work. In spite of its apparent simplicity (or, in fact, because of its simplicity), this turns out to be the formal connection between collective and self-dynamics that best serves the purpose of describing the long-time slow dynamics of systems near their dynamic arrest transitions. It is the best not only because it is the simplest, but also because it turns out to be equally accurate, for the purpose above, as other more sophisticated higher-order Vineyard approximations. For example, given that the SCGLE theory was originally aimed at describing short- and intermediate-time properties, the difference $[C(k,t) - C_S(k,t)]$ was approximated by the difference of the exact short-time/large-k limit $C^{\rm SEXP}(k,t)$ and $C_S^{\rm SEXP}(k,t)$ of these memory functions, for which well established expressions are available in terms of equilibrium structural properties [17, 29, 30]. As was discussed more recently [18], however, an equally accurate approximation is to simply neglect this difference, and to relate the two irreducible memory functions by the simpler relation in equation (2.3).

The third ingredient consists of the independent approximate determination of $F_S(k,t)$ [or $C_S(k,t)$]. One intuitively expects that these k-dependent self-diffusion properties should be simply related to the properties that describe the Brownian motion of individual particles, just like in the Gaussian approximation [2], which expresses $F_S(k,t)$ in terms of the mean-squared displacement $W(t)$ as $F_S(k,t) = \exp[-k^2 W(t)]$. We introduce an analogous approximate connection, but at the level of their respective memory functions. The memory function of $W(t)$ is the so-called time-dependent friction function $\Delta\zeta(t)$. This function, normalized by the free-diffusion friction coefficient ζ_0 ($\equiv k_{\rm B}T/D_0$), is the long-wavelength limit of $C_S(k,t)$, i.e., $\lim_{k\to 0} C_S(k,t) = \Delta\zeta^*(t) \equiv \Delta\zeta(t)/\zeta_0$.

[1] In reality, Nägele *et al* [24] refer to the $[C(k,z)D_0]$ as the 'irreducible memory function', a concept first introduced by Cichocki and Hess [25].

Thus, we interpolate $C_S(k,t)$ between its two exact limits, $C_S(k,t) = C_S^{\rm SEXP}(k,t) + [\Delta\zeta^*(t) - C_S^{\rm SEXP}(k,t)]\lambda(k)$, with $\lambda(k)$ being a phenomenological interpolating function such that $\lambda(k \to 0) = 1$ and $\lambda(k \to \infty) = 0$. In the absence of rigorous fundamental guidelines to construct this interpolating function, we require $\lambda(k)$ to represent the optimum mixing of these two limits of $C_S(k,t)$ in the simplest possible analytical manner. Guided by these practical considerations, in [14] the proposal was made to model $\lambda(k)$ by the functional form $\lambda(k) \equiv [1 + (k/k_{\rm min})^2]^{-1}$, with $k_{\rm min}$ being the position of the first minimum that follows the main peak of the static structure factor $S(k)$. Furthermore, we adopt a simplified version of the interpolation formula above, due to the fact that the present work deals with the long-time slow relaxation processes near the dynamic arrest transition, for which the short-time details described by the short-time memory function $C_S^{\rm SEXP}(k,t)$ are not expected to be relevant. Thus, the interpolating formula above simplifies to

$$C_S(k,t) = \left[\Delta\zeta^*(t)\right]\lambda(k), \tag{2.4}$$

which is incorporated in the present self-consistent theory.

The fourth ingredient of our theory is based on still another exact result, this time for $\Delta\zeta^*(t)$. In [26] the effective Langevin equation of a tracer colloidal particle interacting with the other particles of a mono-disperse suspension was derived, using the concept of contraction of the description [27] (a summary of such a derivation is contained in appendix B of [17]). Besides the solvent friction force, $-\zeta^0\mathbf{V}(t)$, the direct interactions of the tracer particle with the other particles give rise to an additional friction term of the form $-\int_0^t {\rm d}t' \Delta\zeta(t-t')\mathbf{V}(t')$, where $\mathbf{V}(t)$ is the tracer particle's velocity at time t. In the process, an exact result for the time-dependent friction function $\Delta\zeta^*(t) \equiv \Delta\zeta(t)/\zeta^0$ is generated. This exact result may, upon the introduction of two well defined simplifying approximations (referred to as the 'homogeneous fluid' and the 'decoupling' approximations [26]), be converted into the following approximate but general expression:

$$\Delta\zeta^*(t) = \frac{D_0}{3\,(2\pi)^3\, n}\int {\rm d}\mathbf{k}\left[\frac{k[S(k)-1]}{S(k)}\right]^2 F(k,t)F_S(k,t). \tag{2.5}$$

The incorporation of this result finally leads to a closed system of equations, equations (2.1)–(2.5), which constitute the SCGLE theory of colloid dynamics.

Besides the unknown dynamic properties, these equations only involve the static structural property $S(k)$, determined by the methods of equilibrium statistical thermodynamics, and the interpolating function $\lambda(k)$, which also depends on $S(k)$. Notice that the resulting self-consistent scheme is free from any form of adjustable parameters. Let us also mention that equations (2.1) and (2.2) are exact results, and equation (2.5) derives from another exact result. Hence, it should not be a surprise that the same results are employed by other theories; in fact, the same equations are employed in MCT. The difference lies, of course, in the way we relate them and use them. In this sense, the distinctive elements of our theory are the Vineyard-like approximation in equation (2.3) and the interpolating approximation in equation (2.4).

From the SCGLE scheme in equations (2.1)–(2.5) one can derive the equations for its long-time asymptotic solutions. Thus, the unknown dynamic properties $F(k,t)$, $F_S(k,t)$, $C(k,t)$, $C_S(k,t)$, and $\Delta\zeta^*(t)$, which in an ergodic state decay to zero, in a non-ergodic state decay to finite asymptotic values, referred to as the non-ergodicity parameters, that we denote, respectively, by $f(k)S(k)$, $f_S(k)$, $c(k)$, $c_S(k)$, and $\Delta\zeta^{*(\infty)}$. One can then re-write equations (2.1)–(2.5) in terms of these asymptotic values plus a regular contribution that does decay to zero. Taking the long-time limit of the resulting equations leads to a system of five equations for these five unknown non-ergodicity parameters [17, 18]. Such a system of equations can easily be reduced to a single equation for the scalar parameter $\Delta\zeta^{*(\infty)}$, which can be written as

$$\frac{1}{\gamma} = \frac{1}{6\pi^2 n}\int_0^\infty \mathrm{d}k\, k^4 \frac{[S(k)-1]^2\,\lambda^2(k)}{\left[\lambda(k)S(k)+k^2\gamma\right]\left[\lambda(k)+k^2\gamma\right]}, \tag{2.6}$$

with γ defined as $\gamma \equiv D_0/\Delta\zeta^{*(\infty)}$. The parameter γ is just the mean-squared displacement of a particle localized by the arrested cage formed by its neighbors [17]. The form of this criterion exhibits its simplicity: given the effective inter-particle forces, statistical thermodynamic methods allow one to determine $S(k)$, and the absence or existence of *finite* positive real solutions of this equation will indicate if the system remains in the ergodic phase or not (notice that $\gamma = \infty$ is always a solution, representing ergodic states). The meaning of $\sqrt{\gamma}$, as the localization length of a tracer particle in the glass, follows from the fact that the effective force on such tracer particle includes a term given by [26] $\zeta_0 \int_0^\infty \Delta\zeta^*(t-t')\mathbf{v}(t')\,\mathrm{d}t'$; in an arrested state, the non-ergodic part of $\Delta\zeta^*(t)$ generates a harmonic force whose elastic constant, given by $\zeta_0\Delta\zeta^{*(\infty)}$, is related to γ by the definition above, through the equipartition theorem.

The other four equations for the non-ergodicity parameters can then be used to express those quantities in terms of γ. The equations for the non-ergodicity parameters $f(k)$ and $f_S(k)$ then read

$$f(k) = \frac{\lambda(k)S(k)}{\lambda(k)S(k)+k^2\gamma} \tag{2.7}$$

and

$$f_S(k) = \frac{\lambda(k)}{\lambda(k)+k^2\gamma}. \tag{2.8}$$

The last three equations indicate that γ and the non-ergodicity parameters $f(k)$ and $f_S(k)$ only depend on the static structure factor $S(k)$ (and on the interpolating function $\lambda(k)$, which is determined by $S(k)$), and not on transport properties, such as D_0. Thus, they clearly illustrate one important conclusion of the SCGLE theory, namely, that the static structure factor $S(k)$ alone is sufficient to determine if the system will be dynamically arrested or not. In other words, the information needed to decide if the system is arrested is encrypted in $S(k)$, and these three equations provide a practical algorithm to 'de-encrypt' this information. The accuracy of the dynamic arrest scenario thus predicted depends, however, on the quality of the static structure factor $S(k)$ that is fed as an input to the SCGLE theory, in particular to equations (2.6)–(2.8). For this we may resort to any of the available statistical thermodynamic theories to determine $S(k)$ [1]. Here we shall mostly employ the simplest, fully analytic approximation, explained in the following section and in the appendix.

3. Dynamic equivalence between soft and hard spheres

In this section and in the appendix we discuss three related but independent subjects. Taken together, these three subjects define a simple analytic scheme to express the static and dynamic properties of soft-sphere systems in terms of the corresponding properties of the hard-sphere system. The first of these subjects refers to the notion that the static structure of the soft-sphere systems in equation (1.1) must be approximately the same as that of a hard-sphere system with an adequately chosen effective diameter. Taken as an assumption, this notion is referred to as the structural scaling or static equivalence principle. This principle has a dynamic extension, and this is the second subject of this section. Such an extension says that the *dynamic* properties of the soft-sphere systems in equation (1.1) must also be the same as those of the corresponding effective hard-sphere system up to some rescaling prescriptions that we write and illustrate in this section. The third subject refers to the simplest, fully analytic, approximation for the soft-sphere static structure factor $S(k)$ of the systems in equation (1.1), that results when we complement the static equivalence principle above with the Verlet–Weis-improved solution of the Percus–Yevick approximation for hard spheres; the details of this approximation are given in the appendix.

The static equivalence principle is the basis of the treatment of soft cores developed in the framework of the perturbation theory of liquids of Andersen, Weeks and Chandler (AWC [4]; see section 6.3 of [1] for a textbook presentation). In its simplest version, it states that the radial distribution function $g^{(\nu)}(r;n,\sigma^{(\nu)})$ of the soft-sphere system of equation (1.1) with diameter $\sigma^{(\nu)}$ at concentration n is identical to the radial distribution function $g^{(\mathrm{HS})}(r;n,\sigma^{(\mathrm{HS})})$ of a hard-sphere system at *the same* concentration n and with an appropriately chosen diameter $\sigma^{(\mathrm{HS})}$, *except for a small region near* $r = \sigma^{(\nu)}$ (or, without exception, if we describe the static structure in terms of the function $y(r) = \exp(\beta u(r))g(r)$). Conversely, the static structure of the HS system can be represented by the structure of any of the soft-sphere systems in the family described by equation (1.1). As discussed in more detail in the appendix, this expected equivalence can be expressed in terms of the static structure factors $S^{(\nu)}(k;n,\sigma^{(\nu)})$ as the following iso-structurality condition:

$$S^{(\nu)}(k;n,\sigma^{(\nu)}) = S^{(\mathrm{HS})}(k;n,\sigma^{(\mathrm{HS})}), \tag{3.1}$$

with the diameters $\sigma^{(\nu)}$ and $\sigma^{(\mathrm{HS})}$ being related to each other by a more restricted version of this condition such as, for example, $S^{(\nu)}(k_{\max};n,\sigma^{(\nu)}) = S^{(\mathrm{HS})}(k_{\max};n,\sigma^{(\mathrm{HS})})$, with $k_{\max}$ being the position of the main peak of $S(k)$. For moderately soft potentials we shall employ, however, a simpler and more practical relation, referred to as the 'blip function' condition [1], which requires that

$$\int \mathrm{d}^3 r \left[\exp(-\beta u^{(\nu)}(r)) - \exp(-\beta u^{(\mathrm{HS})}(r))\right] = 0. \tag{3.2}$$

It is not difficult to show that the relationship between $\sigma^{(\nu)}$ and $\sigma^{(\mathrm{HS})}$ that results from this condition, for $\beta u^{(\nu)}(r)$ given by equation (1.1), can be written as

$$\left[\frac{\sigma^{(\nu)}}{\sigma^{(\mathrm{HS})}}\right] = \left\{1 - 3\int_0^1 \mathrm{d}x x^2 \exp\left[-\left(\frac{1}{x^{2\nu}} - \frac{2}{x^{\nu}} + 1\right)\right]\right\}^{-\frac{1}{3}}. \tag{3.3}$$

Just as the previous static equivalence is expected to hold on the basis of simple intuitive arguments, one might expect from similar arguments that a dynamic version of this equivalence holds, as discussed and demonstrated in [5] using computer simulated results. Let us now demonstrate that such dynamic equivalence is also built into the SCGLE theory. For this, let us go back to the previous section, to check that the full self-consistent scheme in equations (2.1)–(2.5) needs as the only explicit inputs the number density n (equation (2.5)) and the free-diffusion coefficient $D_0^{(\nu)}$ (equations (2.1), (2.2), and (2.5)) besides the static structure factor $S^{(\nu)}(k; n, \sigma^{(\nu)})$. Then, using the static equivalence condition in equation (3.1) in the self-consistent scheme leads to the conclusion that its solution for $F^{(\nu)}(k, t; n, \sigma^{(\nu)})$ and $F_S^{(\nu)}(k, t; n, \sigma^{(\nu)})$ must satisfy the referred extension, which can be written as

$$F^{(\nu)}(k, D_0^{(\nu)}t; n, \sigma^{(\nu)}) = F^{(\mathrm{HS})}(k, D_0^{(\mathrm{HS})}t; n, \sigma^{(\mathrm{HS})}) \tag{3.4}$$

and

$$F_S^{(\nu)}(k, D_0^{(\nu)}t; n, \sigma^{(\nu)}) = F_S^{(\mathrm{HS})}(k, D_0^{(\mathrm{HS})}t; n, \sigma^{(\mathrm{HS})}). \tag{3.5}$$

This correspondence between soft- and hard-sphere systems implies that all the soft-sphere systems in the family in equation (1.1) are structurally and dynamically identical to each other, in the sense that they share not only the same static structure factor $S(k)$, but also the same dynamic properties. Hence, the structure and dynamics of any member of this family can be used to represent the structure and the dynamics of any other member, including, of course, the HS system itself.

The dynamic equivalence indicated in equations (3.4) and (3.5) is meant to apply at all times and wavevectors; in particular it should apply in the asymptotic long-time regime described by the equations for the squared localization length γ, equation (2.6), and for the non-ergodicity parameters, equations (2.7) and (2.8), which then must be such that

$$\gamma^{(\nu)}(n, \sigma^{(\nu)}) = \gamma^{(\mathrm{HS})}(n, \sigma^{(\mathrm{HS})}), \tag{3.6}$$

$$f^{(\nu)}(k; n, \sigma^{(\nu)}) = f^{(\mathrm{HS})}(k; n, \sigma^{(\mathrm{HS})}), \tag{3.7}$$

and

$$f_S^{(\nu)}(k; n, \sigma^{(\nu)}) = f_S^{(\mathrm{HS})}(k; n, \sigma^{(\mathrm{HS})}). \tag{3.8}$$

An immediate consequence of these results is that two soft-sphere systems with diameters $\sigma^{(\nu)}$ and $\sigma^{(\nu')}$ related by the blip function condition will have the same glass transition number concentration, $n_{\mathrm{g}}^{(\nu)} = n_{\mathrm{g}}^{(\nu')} = n_{\mathrm{g}}$. Their respective volume fractions, however, will differ and will be such that $\phi_{\mathrm{g}}^{(\nu)} = [\sigma^{(\nu)}/\sigma^{(\nu')}]^3 \phi_{\mathrm{g}}^{(\nu')}$. In particular, the glass transition volume fraction $\phi_{\mathrm{g}}^{(\nu)}$ of any soft-sphere system can be written as

$$\phi_{\mathrm{g}}^{(\nu)} = [\sigma^{(\nu)}/\sigma^{(\mathrm{HS})}]^3 \phi_{\mathrm{g}}^{(\mathrm{HS})}. \tag{3.9}$$

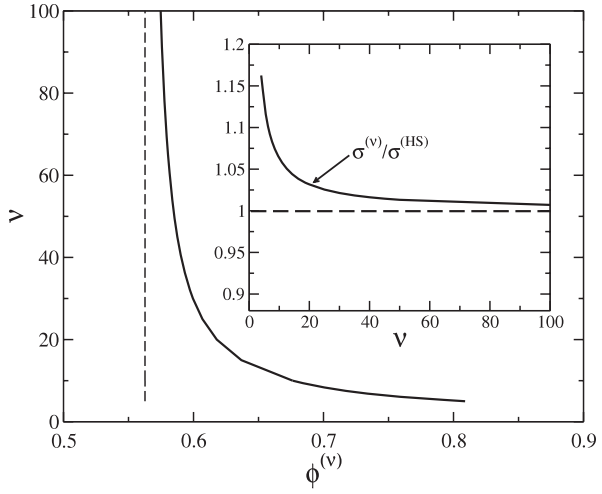

Figure 1. Dynamic arrest phase diagram of the soft-sphere systems in equation (1.1) in the softness–concentration state space. The solid line is the glass transition line when the concentration n is scaled as the volume fraction $\phi^{(\nu)} = \pi n \sigma^{(\nu)3}/6$. The ergodic and the arrested states lie, respectively, to the left and to the right of this line. The inset plots the dependence of the ratio $[\sigma^{(\nu)}/\sigma^{(\mathrm{HS})}]$ on the softness parameter ν, given by equation (3.3). The dashed vertical line in the main figure represents the asymptotic value $\phi_{\mathrm{g}}^{(\mathrm{HS})} = \lim_{\nu\to\infty} \phi_{\mathrm{g}}^{(\nu)} = 0.563$; according to the assumption of dynamic equivalence, this line would be the glass transition line if the horizontal axis were labeled not by $\phi^{(\nu)}$ but by the number concentration n (or, equivalently, by the effective volume fraction $\phi^{(\mathrm{HS})} = \pi n \sigma^{(\mathrm{HS})3}/6$).

Since we know the value of $\phi_{\mathrm{g}}^{(\mathrm{HS})}$ (=0.575 according to experiment [31]; 0.563 according to the present theory [18]), and since the ratio $[\sigma^{(\nu)}/\sigma^{(\mathrm{HS})}]$ is given by equation (3.3) (see the inset of figure 1), we can immediately predict the value of the glass transition volume fraction $\phi_{\mathrm{g}}^{(\nu)}$ for any soft potential. In this manner, we can draw the glass transition line in the concentration–softness state space, as is done in figure 1, where the solid line corresponds to the loci of the points $(\phi_{\mathrm{g}}^{(\nu)}, \nu)$. The points $(\phi^{(\nu)}, \nu)$ to the left of this line represent ergodic states, whereas the arrested states lie in the region to the right of this glass transition line. Of course, if instead of the volume fraction $\phi^{(\nu)}$ we had used the concentration n to label the horizontal axis in this figure, the glass transition line would be a vertical line, since, as indicated above, $n_{\mathrm{g}}^{(\nu)} = n_{\mathrm{g}}^{(\nu')} = n_{\mathrm{g}}$. For example, if the horizontal axis of figure 1 were labeled not by $\phi^{(\nu)}$ but by $[\sigma^{(\mathrm{HS})}/\sigma^{(\nu)}]^3 \phi^{(\nu)} = \phi^{(\mathrm{HS})} = \pi n \sigma^{(\mathrm{HS})3}/6$, the glass transition line would be the dashed line in this figure.

Another important result of the dynamic equivalence being discussed is explicitly expressed by equation (3.6), which states that the localization length squared $\gamma^{(\nu)}(n, \sigma^{(\nu)})$ of a soft-sphere system at concentration n does not depend on the softness of the potential, and is, hence, the same as that of the hard-sphere system at the same concentration (provided that the diameters $\sigma^{(\nu)}$ and $\sigma^{(\mathrm{HS})}$ are related by the blip function condition). An immediate consequence of this equality involves the Lindemann ratio, defined as $r_{\mathrm{L}}^{(\nu)}(n) \equiv \sqrt{\gamma^{(\nu)}}/n^{-1/3}$: equation (3.6) implies that $r_{\mathrm{L}}^{(\nu)}(n) = r_{\mathrm{L}}^{(\mathrm{HS})}(n)$, i.e., that the Lindemann ratio does not depend on the softness of the pair potential. This means that a universal Lindemann's

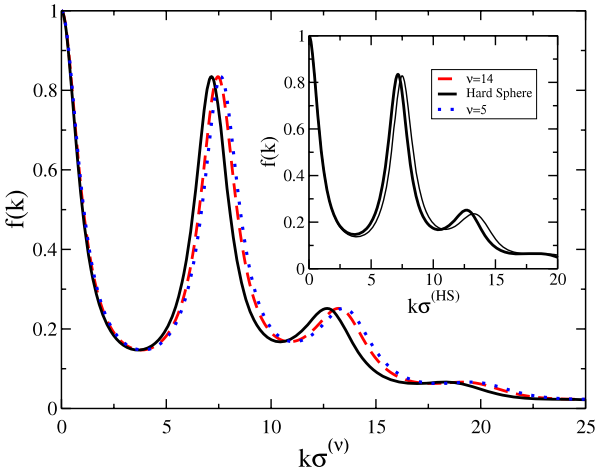

Figure 2. Non-ergodicity parameter $f^{(\nu)}(k;n,\sigma^{(\nu)})$ plotted as a function of $k\sigma^{(\nu)}$ (main figure) and of $k\sigma^{(\mathrm{HS})}$ (inset) for the systems with softness parameter $\nu=\infty$(HS), 14, and 5 (solid, dashed, and dotted lines, respectively), at the ideal glass transition volume fraction $\phi_{\mathrm{g}}^{(\nu)}$. The input static structure factor $S^{(\nu)}(k;n,\sigma^{(\nu)})$ used in equations (2.6) and (2.7) was approximated according to the simple analytic scheme based on the static equivalence principle plus the Percus–Yevick/Verlet–Weis approximation (appendix). By construction, the three curves collapse exactly onto the HS curve when plotted as a function of $k\sigma^{(\mathrm{HS})}$ (the solid line of the inset). For comparison, the HS result obtained with Rogers–Young's static structure factor (see section 4) is shown as a thin solid line in the inset.

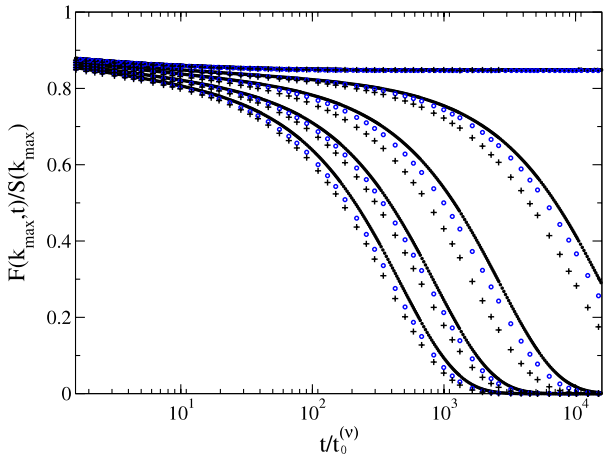

Figure 3. Collective correlator $f(k,t)\equiv F(k,t)/S(k)$ as a function of time in units of $t_0^{(\nu)}\equiv\sigma^{(\nu)2}/D_0$ at fixed $k=k_{\max}$ for the soft-sphere systems in equation (1.1) with $\nu=\infty$(HS), 14, and 5, in the vicinity of their glass transition. The solid lines from left to right correspond to the HS system at $\phi^{(\mathrm{HS})}=0.559$, 0.56, 0.561, 0.562, and $0.563(=\phi_{\mathrm{g}}^{(\mathrm{HS})})$. The circles and crosses correspond, respectively, to $\nu=14$ and 5, at the equivalent volume fractions $\phi^{(\nu)}=[\sigma^{(\nu)}/\sigma^{(\mathrm{HS})}]^3\phi^{(\mathrm{HS})}$ with $[\sigma^{(14)}/\sigma^{(\mathrm{HS})}]=1.045$ and $[\sigma^{(5)}/\sigma^{(\mathrm{HS})}]=1.129$ determined by equation (3.3). The circles and crosses will collapse onto the solid lines if the time is expressed in units of $t_0^{(\mathrm{HS})}\equiv\sigma^{(\mathrm{HS})2}/D_0$.

rule emerges from these considerations, namely, that all the glasses made of soft-sphere particles melt when $r_{\mathrm{L}}^{(\nu)}(n_{\mathrm{g}})=r_{\mathrm{L}}^{(\mathrm{HS})}(n_{\mathrm{g}})=0.105$, with the numerical value being another prediction of the present theory [17].

The equality of the non-ergodicity parameters in equations (3.7) and (3.8) above expresses an expected independence of $f^{(\nu)}(k;n,\sigma^{(\nu)})$ and $f_S^{(\nu)}(k;n,\sigma^{(\nu)})$ from the softness parameter ν when plotted as a function of the unscaled wavevector k (or as a function of k scaled with a ν-independent typical length, such as $\sigma^{(\mathrm{HS})}$). By construction, this scaling is exactly satisfied when the input static structure factor $S^{(\nu)}(k;n,\sigma^{(\nu)})$ used in equations (2.6) and (2.7) is based precisely on the static equivalence principle, as the analytic scheme involving the Percus–Yevick/Verlet–Weis approximation in the appendix is. We illustrate this in figure 2, where the non-ergodicity parameters $f^{(\nu)}(k;n,\sigma^{(\nu)})$ of the soft-sphere systems interacting through a hard-sphere ($\nu=\infty$), a moderately soft ($\nu=14$), and a soft ($\nu=5$) potential are plotted as a function of the wavevector k scaled with the corresponding soft-sphere diameter $\sigma^{(\nu)}$ (main figure). The same information is then plotted in the inset as a function of $k\sigma^{(\mathrm{HS})}$, where the three results collapse exactly onto a single curve corresponding to the non-ergodicity parameter of the hard-sphere system (solid curve). We notice that the wavevector shift from the hard-sphere limit in the main figure is rather small but appreciable. This simple approximate scheme to calculate the non-ergodicity parameters satisfies exactly the result in equation (3.9), with $\phi_{\mathrm{g}}^{(\mathrm{HS})}=0.563$ and with $\phi_{\mathrm{g}}^{(\nu)}/\phi_{\mathrm{g}}^{(\mathrm{HS})}=[\sigma^{(\nu)}/\sigma^{(\mathrm{HS})}]^3$ determined by the blip function result in equation (3.3); this yields $\phi_{\mathrm{g}}^{(14)}=0.643$, and $\phi_{\mathrm{g}}^{(5)}=0.8089$.

Let us finally discuss the full dynamic equivalence expressed by equations (3.4) and (3.5) above. The first of these equations, along with equation (3.1), may be rewritten in terms of the propagators $f^{(\nu)}(k,D_0^{(\nu)}t;n,\sigma^{(\nu)})\equiv F^{(\nu)}(k,D_0^{(\nu)}t;n,\sigma^{(\nu)})/S^{(\nu)}(k;n,\sigma^{(\nu)})$ as

$$f^{(\nu)}(k,D_0^{(\nu)}t;n,\sigma^{(\nu)})=f^{(\mathrm{HS})}(k,D_0^{(\mathrm{HS})}t;n,\sigma^{(\mathrm{HS})}). \quad (3.10)$$

This means that the collective propagator $f^{(\nu)}(k,D_0^{(\nu)}t;n,\sigma^{(\nu)})$ at a given n and for fixed k will decay identically to the propagator of the hard-sphere system, except for a trivial rescaling of the time due to possible differences in the short-time diffusion coefficients $D_0^{(\nu)}$ and $D_0^{(\mathrm{HS})}$. In figure 3 we present the temporal relaxation of the propagator $f^{(\mathrm{HS})}(k_{\max},D_0^{(\mathrm{HS})}t;n,\sigma^{(\mathrm{HS})})$ of the hard-sphere system at the position $k_{\max}$ of the first maximum of $S(k)$ and in the vicinity of the glass transition, i.e. for the sequence of volume fractions $\phi^{(\mathrm{HS})}=0.559$, 0.560, 0.561, 0.562, and $0.563\ (=\phi_{\mathrm{g}}^{(\mathrm{HS})})$ (solid curves, from left to right). According to equation (3.10), and assuming that $D_0^{(\nu)}=D_0^{(\mathrm{HS})}=D_0$, exactly the same solid curves would also represent the decay of $f^{(\nu)}(k,D_0t;n,\sigma^{(\nu)})$ of any soft-sphere system with arbitrary ν but the same concentration and wavevector, when plotted as a function of the time scaled in the same time unit $t_0^{(\mathrm{HS})}\equiv\sigma^{(\mathrm{HS})2}/D_0^{(\mathrm{HS})}$. If, however, we plot $f^{(\nu)}(k,D_0^{(\nu)}t;n,\sigma^{(\nu)})$ as a function of the time scaled with $t_0^{(\nu)}\equiv\sigma^{(\nu)2}/D_0^{(\nu)}$, then the curves for the different soft-sphere systems are shifted with respect to each other, as illustrated in figure 3.

In experiment, theory, and simulation, one normally expresses the dynamic and static properties of a given (hard

or soft) system in terms of properties scaled with the typical times and lengths of that particular system. The use of different time and length scales for different systems obscures a little the neat equivalence just discussed. Nevertheless, this equivalence may also be enunciated as simple scaling rules for the static and dynamic properties. To illustrate this, let us use a scaled notation in which the propagator $f^{(\nu)}(k, D_0^{(\nu)}t; n, \sigma^{(\nu)})$ is written as $f^{(\nu)}(k, D_0^{(\nu)}t; n, \sigma^{(\nu)}) = \hat{f}^{(\nu)}(y, \tau; \phi^{(\nu)})$ with $y \equiv k\sigma^{(\nu)}$ and $\tau \equiv t/t_0^{(\nu)}$. With this notation, equation (3.10) can also be written as

$$\hat{f}^{(\nu)}(y, \tau; \phi^{(\nu)}) = \hat{f}^{(\mathrm{HS})}(\delta_\nu^{-1} y, \eta_\nu \delta_\nu^2 \tau; \delta_\nu^{-3}\phi^{(\nu)}) \qquad (3.11)$$

where $\delta_\nu \equiv [\sigma^{(\nu)}/\sigma^{(\mathrm{HS})}]$ and $\eta_\nu \equiv [D_0^{(\nu)}/D_0^{(\mathrm{HS})}]$. This means that if we have determined the full-time and wavevector dependence of the collective propagator $\hat{f}^{(\mathrm{HS})}(y, \tau; \phi^{(\nu)})$ of the hard-sphere system (as we can do within the SCGLE theory [17]), then we have also determined the dynamics of any soft-sphere system in its own scaled variables up to the simple scaling rule given by this equation.

4. Comparison with experimental data

Let us now test the practical use of this simple scheme by means of its comparison with the experimentally measured dynamic properties of dispersions of moderately soft particles. Since the use of this scheme involves the dynamic properties of the reference hard-sphere system, let us first assess its accuracy when applied to such a reference system; i.e., let us compare the solutions of the SCGLE theory for the HS system, such as those plotted in figure 3, with the actual experimental data of van Megen and Underwood [31]; such a comparison, which complements those initiated in [16, 17], is presented in figure 4. Let us stress that this is a direct and straightforward comparison between the full time-dependent solution of the SCGLE theory and the corresponding experimental data. In contrast with similar comparisons involving MCT, the present comparison does not involve approximate asymptotic expressions for the intermediate scattering function in specific regimes, nor the use of the corresponding adjustable parameters, since our interest here is to see the capability of our theory to describe the full-time dependence actually observed in the experiments.

The glass transition of the hard-sphere system occurs, according to the experimental report, at the volume fraction $\phi_g = 0.575$ [31]. The SCGLE theory, on the other hand, predicts the dynamic glass transition to occur at $\phi_g = 0.563$. Thus, in figure 4 we compare the results of the SCGLE theory with the experimental results at the same separation parameter $\epsilon \equiv \frac{\phi - \phi_g}{\phi_g}$. This means that the theoretical curves in the figure, corresponding to the sequence of volume fractions $\phi = 0.485$, 0.517, 0.524, 0.562, 0.569, and 0.575, are being compared with the experimental sequence of experimental volume fractions $\phi = 0.494$, 0.528, 0.535, 0.574, 0.581, and 0.587, both corresponding to the same sequence of separation parameters $\epsilon = -0.141$, -0.082, -0.069, -0.002, 0.01, and 0.021.

In order to establish this comparison of the theoretical results with the experimental data a value had to be given to the scaling time $t_0 \equiv \sigma^2/D_0$, a value that must reflect, among other

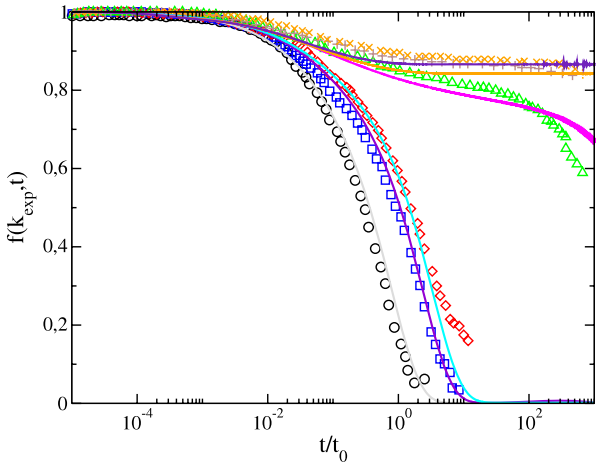

Figure 4. Comparison of the SCGLE collective correlator $f(k, t) \equiv F(k, t)/S(k)$ of the hard-sphere system at the position $k_{\max}$ of the main peak of $S(k)$ (solid lines) with the experimental results of van Megen and Underwood [31] (symbols) corresponding to the experimental volume fractions $\phi = 0.494$, 0.528, 0.535, 0.574, 0.581, and 0.587 (from bottom to top). The SCGLE theory predicts $\phi_g = 0.563$, and hence the comparison is made at the same values of the separation parameter $\epsilon = (\phi - \phi_g)/\phi_g$.

factors, the intensity of hydrodynamic interactions. The effects of these interactions are actually quite important in the short-time dynamics of hard-sphere dispersions at these high volume fractions. Although there is no rigorous treatment of the detailed manner in which hydrodynamic interactions will affect the long-time relaxation near the glass transition, a reasonable expectation is that these effects will only renormalize D_0 [13], and hence, also t_0. Thus, at this stage, we simply assume that these effects may be taken into account by the SCGLE theory through an effective value of this scaling time, which we then treat as an adjustable parameter. Furthermore, we neglect its possible dependence on volume fraction within the experimental range reported in the figure. In this manner, we determined t_0 by shifting the theoretical results for the lowest volume fraction $\phi = 0.494$ in figure 4 to coincide with the corresponding experimental data. This yields a value $t_0 \cong 0.286$ s, which was then employed in the comparisons at the other volume fractions reported in the figure. Clearly, the relaxation of the collective correlator of the three states with the lowest volume fraction in figure 4 (which are in the metastable liquid regime) are fitted quite acceptably. The two states with the highest volume fraction are on the glass side and have high non-ergodicity parameters. Nevertheless, although the differences cannot be fully appreciated, we believe that our theoretical predictions give at least a good first-order quantitative approximation to the experimental values. The remaining state in figure 4, phi $= 0.574$, which indeed is on the fluid side but very close to the glass, does show the typical two-step decay, but the height of the plateau and the timescale of the alpha-relaxation are a bit off. This figure illustrates the overall level of agreement of our simple theoretical scheme with the experimental results for hard spheres, which we find quite good, considering that it covers the whole experimentally recorded time and concentration regimes and

that such comparison involved only one adjustable parameter, t_0, to adjust the timescale, plus the empirical mechanism to adjust the volume fraction so that the glass transition is located at a common value, $\epsilon = 0$, of the separation parameter $\epsilon \equiv \frac{\phi-\phi_g}{\phi_g}$. We must also mention, however, that it is at the position of the main peak of $S(k)$ where the agreement between the measured and the theoretically predicted long time is best. At other wavevectors the agreement deteriorates to the same degree that the agreement between the theoretical and the measured non-ergodicity parameters $f(k)$ deteriorates, as discussed in [17].

Let us now perform a similar comparison between the present theoretical scheme and the experimental data of a moderately soft-sphere system, namely, the dispersion of microgel particles studied by Bartsch *et al* [10] around its ergodic–non-ergodic transition. These authors indicate a value of the soft-sphere diameter $\sigma^{(\nu)}$ of 1.0 μm, and report the glass transition to occur at a volume fraction $\phi_g^{(\nu)} \cong 0.644$. Unfortunately, they do not define or quantify the degree of softness of these particles, in a manner that serves us to determine the parameter ν of our present model. We may use, however, the phase diagram in figure 1 to estimate this parameter by looking at the value of ν whose glass transition volume fraction $\phi_g^{(\nu)}$ is the closest to the experimentally reported value of 0.644. From the results in figure 1 we have that $\phi_g^{(14)} \cong 0.643$. Thus, we assume that $\nu = 14$ is the value of the softness parameter that best represents the experimental system. We then compare the properties of the soft-sphere system of the family in equation (1.1) with $\nu = 14$ with the experimental data of Bartsch *et al* [10]. Notice that, since the experimental and the theoretical glass transition volume fractions coincide by construction, there is no need to use the separation parameter to compare experimental data and theoretical results. To calculate the latter we have used the static inputs calculated with the simple approximation for $S^{(\nu)}(k)$ described in the appendix. The resulting comparison is contained in figure 5. Just like in the hard-sphere case, here too we treated t_0 as an adjustable parameter. Thus, using the experimental and theoretical data of the sample with volume fraction $\phi = 0.642$, just before the glass transition, we determine the value $t_0 \cong 3.5 \times 10^{-2}$ s. The same value of t_0 was then employed at the other volume fractions. Once again the comparison is very good in absolute terms, but also considering the simplicity of the theoretical scheme employed in the analysis of the static and the time-dependent properties of the system.

Let us finally mention that the estimate of the softness parameter above may be subjected to a small correction. The reason for this is that, if instead of the theoretical value of the hard-sphere glass transition $\phi_g^{(HS)} = 0.563$ employed in the procedure above, we had employed the experimental value, $\phi_g^{(HS)} = 0.575$, we would have obtained a slightly larger value of the softness parameter, namely, $\nu \approx 16.5$. In this procedure, the comparison of the theoretical results with the experimental data in figure 5 needs to be done at the same value of the separation parameter, as in the hard-sphere case discussed above. The quality of the resulting comparison between theoretical predictions and experimental data is, however, exactly the same as in figure 5.

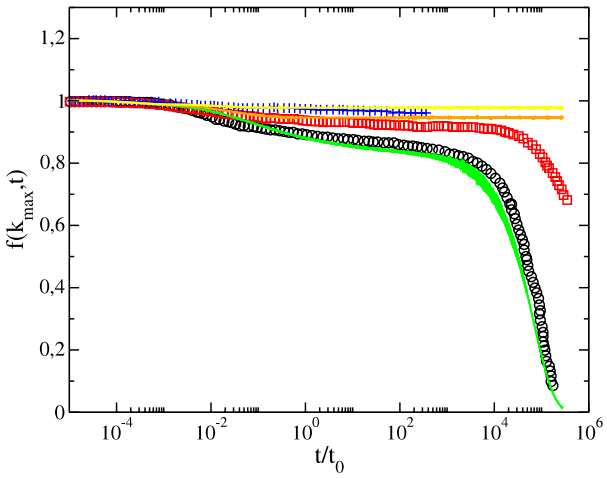

Figure 5. Comparison of the SCGLE collective correlator $f(k,t) \equiv F(k,t)/S(k)$ of the soft-sphere system in equation (1.1) with $\nu = 14$ at the position k_{max} of the main peak of $S(k)$ in the vicinity of the glass transition, for the volume fractions $\phi^{(14)} \equiv \pi n \sigma^{(14)3}/6 = 0.642$, 0.667, and 0.7 (from bottom to top, solid lines). The symbols are the corresponding experimental results of Bartsch *et al* [10] at the same volume fractions.

5. Very soft potentials

The comparison in section 4 of the simple theoretical scheme discussed in section 3 with experimental data illustrates the quantitative accuracy of that scheme to describe dynamic arrest in systems with moderately soft potentials, like those of equation (1.1) with ν larger than or of the order of 10. This scheme, however, is expected to fail for sufficiently soft interactions, and a natural question refers to its regime of validity and its degree of failure when applied to softer potentials, and this is the subject of the present section. For example, one wonders to what extent the scaling rules discussed in section 3 will be satisfied if the simple analytic approximation for $S^{(\nu)}(k; n, \sigma^{(\nu)})$ employed in that discussion is replaced, in the absence of systematic computer simulation results, by an independent approximation for the static structure factor which does not have the static equivalence property built into its definition.

To check this, here we resort to the Rogers–Young closure of the Ornstein–Zernike equation for the soft-sphere potentials of equation (1.1), which we numerically solve for $\hat{S}^{(\nu)}(k\sigma^{(\nu)}; \phi^{(\nu)}) \equiv S^{(\nu)}(k; n, \sigma^{(\nu)})$. The first question is then if the resulting static structure factors satisfy the simple version of the static equivalence principle, discussed in section 3. This is defined by the iso-structurality condition $S^{(\nu)}(k; n, \sigma^{(\nu)}) = S^{(HS)}(k; n, \sigma^{(HS)})$ in equation (3.1), that requires both (soft- and hard-sphere) equivalent systems to have *the same* number concentration, and the ratio $[\sigma^{(\nu)}/\sigma^{(HS)}]$ to be determined by means of the blip function result in equation (3.3).

We may define the same structural scaling principle in a less restrictive fashion than that involved in equation (3.1) of section 3. For this we use the function $y(r) = e^{-\beta u(r)} g(r)$, so that instead of equation (3.1) we write

$$y^{(\nu)}(r; n^{(\nu)}, \sigma^{(\nu)}) = y^{(HS)}(r; n^{(HS)}, \sigma^{(HS)}), \qquad (5.1)$$

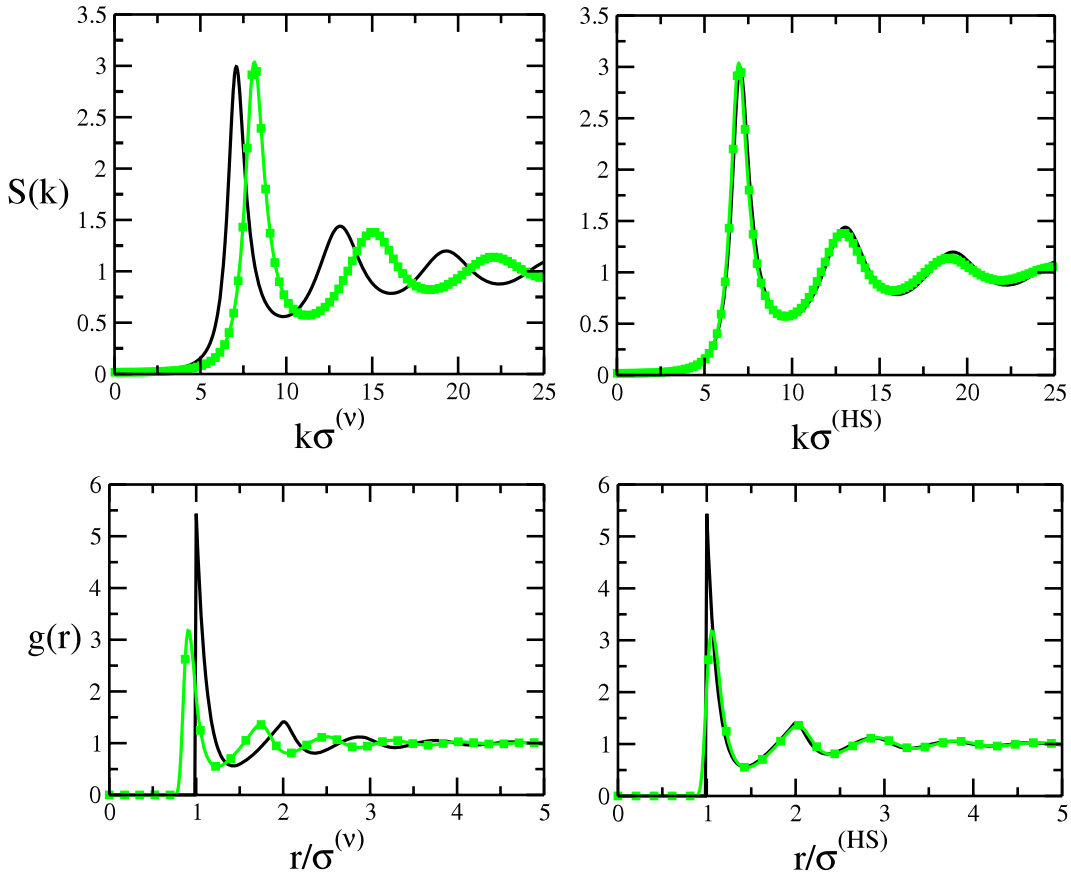

Figure 6. Static structure factor $S(k)$ (upper row) and radial distribution function $g(r)$ (lower row) of a hard-sphere system at $\phi^{(\mathrm{HS})} = 0.5$ (solid dark lines) and of a soft-sphere system with $\nu = 5$ at $\phi^{(5)} = 0.79$ (squares with green lines) calculated within the Rogers–Young approximation, and plotted as a function of the variables scaled with the soft-sphere diameter (left column) and with a common length scale, for which we use $\sigma^{(\mathrm{HS})}$ (right column).

in which we no longer require *a priori* the two structurally equivalent systems to have the same number concentration n. Instead, we state the structural scaling principle in terms of the requirement that for any soft-sphere system with given number concentration $n^{(\nu)}$ and soft-sphere diameter $\sigma^{(\nu)}$, whose function $y(r)$ is $y^{(\nu)}(r; n^{(\nu)}, \sigma^{(\nu)})$, there will be an effective hard-sphere system with a number concentration $n^{(\mathrm{HS})}$ and diameter $\sigma^{(\mathrm{HS})}$, generally different from $n^{(\nu)}$ and $\sigma^{(\nu)}$, whose function $y^{(\mathrm{HS})}(r; n^{(\mathrm{HS})}, \sigma^{(\mathrm{HS})})$ will be identical to that of the soft-sphere system at the *same* distance r. The condition in equation (5.1) can also be stated in terms of the radial distribution functions $g(r)$, except in the neighborhood of $r = \sigma^{(\mathrm{HS})}$, which is the only distance where the softness of the potential manifests itself more dramatically. Thus, we expect that the values near the contact of $g(r)$ will be very different for different softness parameters ν, but the rest of the function will be almost identical. Similarly, we expect that the $S(k)$ of structurally equivalent soft systems will be identical at the main peak but not all larger wavevectors. These differences will be more appreciable for the softest potentials. One of the aims of this section is to determine these differences.

In order to fully define this less restrictive version of the static equivalence principle we must indicate the procedure to determine the effective hard-sphere diameter $\sigma^{(\mathrm{HS})}$ and concentration $n^{(\mathrm{HS})}$. For this, let us consider the general structural equivalence condition of equation (5.1) at the position $k_{\max}$ of the main peak of the static structure factor, and let us write it in terms of dimensionless variables as $\hat{S}^{(\nu)}(k_{\max}\sigma^{(\nu)}; \phi^{(\nu)}) = \hat{S}^{(\mathrm{HS})}(k_{\max}\sigma^{(\mathrm{HS})}; \phi^{(\mathrm{HS})})$. In order to use this condition we choose an arbitrary volume fraction $\phi^{(\nu)}$ of the soft-sphere system with softness parameter ν to calculate $\hat{S}^{(\nu)}(k_{\max}\sigma^{(\nu)}; \phi^{(\nu)})$ within the RY approximation to determine the height of the main peak of the static structure factor. We then compute $\hat{S}^{(\mathrm{HS})}(k\sigma^{(\mathrm{HS})}; \phi^{(\mathrm{HS})})$ for the hard-sphere system, also within the RY approximation, varying $\phi^{(\mathrm{HS})}$ until $\hat{S}^{(\mathrm{HS})}(k_{\max}\sigma^{(\mathrm{HS})}; \phi^{(\mathrm{HS})})$ matches the height of the main peak of the static structure factor of the soft system; this determines the ratio $[\phi^{(\mathrm{HS})}/\phi^{(\nu)}]$. Thus, these two static structure factors now coincide in the height, but not in the positions $k_{\max}\sigma^{(\nu)}$ and $k_{\max}\sigma^{(\mathrm{HS})}$, of the main peak of $S(k)$. These positions, however, are shifted by a factor given precisely by the ratio $[\sigma^{(\mathrm{HS})}/\sigma^{(\nu)}]$, and hence the measurement of this shift determines the desired diameter ratio. From the ratios $[\phi^{(\mathrm{HS})}/\phi^{(\nu)}]$ and $[\sigma^{(\mathrm{HS})}/\sigma^{(\nu)}]$ thus determined we may also evaluate the $[n^{(\mathrm{HS})}/n^{(\nu)}]$, since these ratios are related by

$$\left[\frac{\phi^{(\nu)}}{\phi^{(\mathrm{HS})}}\right]\left[\frac{\sigma^{(\mathrm{HS})}}{\sigma^{(\nu)}}\right]^3 = \left[\frac{n^{(\nu)}}{n^{(\mathrm{HS})}}\right]. \tag{5.2}$$

These concepts are illustrated in figure 6 with the RY results for the static structure factor $\hat{S}^{(\nu)}(k_{\max}\sigma^{(\nu)}; \phi^{(\nu)})$ of a hard-sphere ($\nu = \infty$) and of a soft-sphere ($\nu = 5$) system with

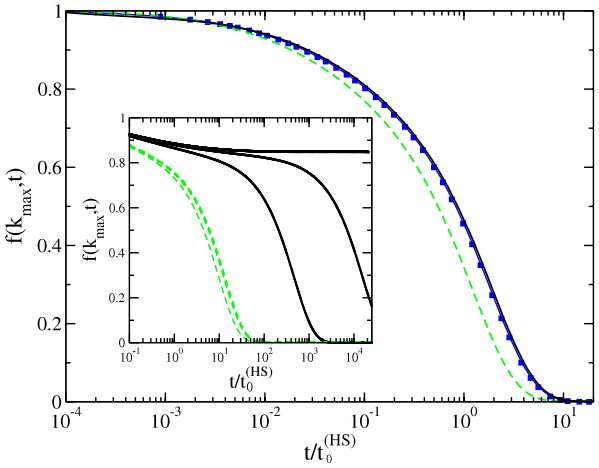

Figure 7. Collective propagators of three statically equivalent systems: a hard-sphere system at $\phi^{(\mathrm{HS})} = 0.5$ (dark solid lines), a soft-sphere system with $\nu = 5$ at $\phi^{(5)} = 0.79$ (red dashed lines), and a soft-sphere system with $\nu = 14$ at $\phi^{(14)} = 0.575$ (blue line with squares) calculated with the SCGLE theory using Rogers–Young input static structure factors. In the inset a similar comparison is made between the first two of these systems at volume fractions very close to the hard-sphere glass transition, corresponding to $\phi^{(\mathrm{HS})} = 0.54877$, 0.55172, and 0.5527. We notice that the HS glass transition volume fraction predicted by the SCGLE theory using Rogers–Young static inputs is $\phi_{\mathrm{g}}^{(\mathrm{HS})} = 0.5524$.

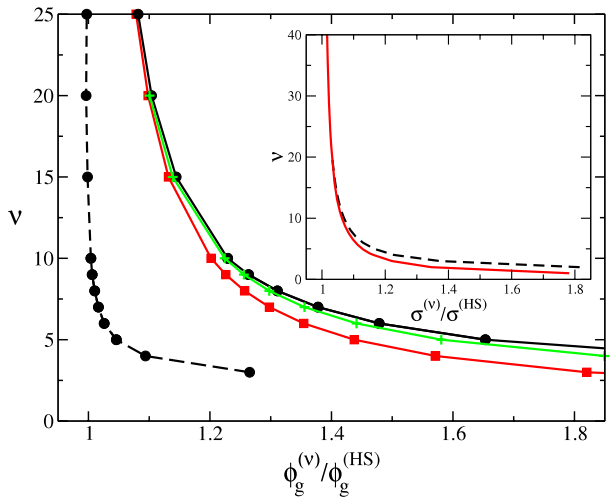

Figure 8. Glass transition line normalized with its hard-sphere limit. The circles were obtained using the Rogers–Young structure factor directly in the SCGLE theory, and the squares were obtained using the analytic scheme for the structure factor described in the appendix. In the inset we show the differences between the ratio $\sigma^{(HS)}/\sigma^{(\nu)}$ calculated with the blip function method (the solid line) and with the iso-structurality condition described in the text (the dashed line). The predictions for the glass transition with the latter method are represented by the crosses. On the extreme left we plot the results for the ratio $n_{\mathrm{g}}^{(\nu)}/n_{\mathrm{g}}^{(HS)}$ calculated with the Rogers–Young inputs.

volume fractions adjusted to have the same height $S(k_{\max})$ of the main peak. Matching this height determines a unique value for the ratio $[\phi^{(\mathrm{HS})}/\phi^{(\nu)}]$, which in this case is $[0.50/0.79] = 0.633$. We may now determine the ratio $[\sigma^{(\mathrm{HS})}/\sigma^{(\nu)}]$ by measuring the ratio $[k_{\max}\sigma^{(\mathrm{HS})}/k_{\max}\sigma^{(\nu)}]$, which in this particular case is $[\sigma^{(\mathrm{HS})}/\sigma^{(\nu)}] = [k_{\max}\sigma^{(\mathrm{HS})}/k_{\max}\sigma^{(\nu)}] = 0.859$. In the same figure we re-plot these static structure factors now as a function of the wavevector scaled with the same length scale, namely, the hard-sphere diameter $\sigma^{(\mathrm{HS})}$ (right column of the figure). There we see that this rescaling of the wavevector not only leads to the overlap of the main peak, but also to a very close coincidence at most wavevectors. The main differences are observed in the height of the subsequent maxima of $S(k)$ at larger wavevectors. The same comparison, but now in terms of the radial distribution functions, is included in the lower row of this figure. There we notice that, in spite of the expected differences near the distance of closest approach, the long-range oscillations of $g(r)$ of both systems coincide almost exactly. This means that the structural equivalence will also imply the equivalence of properties that do not depend crucially on the value of $g(r)$ near the distance of closest approach, such as the integral of $g(r)$, that determines the isothermal compressibility according to the compressibility equation.

Going back to equation (5.2), let us use the results of this procedure to evaluate the ratio of number concentrations, with the result that $[n^{(\nu)}/n^{(\mathrm{HS})}] \approx 1$. This then means that the same simple structural scaling principle, employed in section 3 to define the analytic approximation of the structure of soft-sphere systems in terms of the PY–VW structure of the hard-sphere model, turns out to hold also when the structure of these systems is described by the RY approximation. The main difference is, however, that in the present case we did not use the blip function method, and that the approximate equality $n^{(\nu)} \approx n^{(\mathrm{HS})}$ is a result and not an *a priori* assumption of the method.

The next question is to what extent this static structural equivalence extends over to the dynamic domain. To investigate this, we now use the two equivalent static structure factors, $\hat{S}^{(\nu)}(k_{\max}\sigma^{(\nu)}; \phi^{(\nu)})$ and $\hat{S}^{(\mathrm{HS})}(k_{\max}\sigma^{(\mathrm{HS})}; \phi^{(\mathrm{HS})})$, as static inputs of the SCGLE theory. In this manner we determine the dynamic properties of both systems to check if they coincide, as expected on the basis of the arguments given in section 3. The answer is illustrated by the results in figure 7, where we plot the collective propagator $f(k,t)$ of the hard-sphere system at $\phi^{(\mathrm{HS})} = 0.5$ and of two statically equivalent soft-sphere systems with $\nu = 5$ and 14 calculated with the SCGLE theory using the Rogers–Young input static static structure factors. Clearly from the comparison in the main figure we learn that even though the three systems are structurally equivalent in the sense illustrated in figure 6, they do not yield the same dynamics. The corresponding deviations are in fact negligible for the moderately soft potential ($\nu = 14$), but they are definitely appreciable in the case of the very soft potential ($\nu = 5$).

The state illustrated in the main figure in figure 7 is relatively far from the glass transition. The inset shows a similar comparison between the HS system and the system with the softer potential ($\nu = 5$) for two volume fractions slightly below, and one volume fraction slightly above, the HS glass transition. This comparison illustrates the fact the scenario offered by the structurally equivalent static structure factors of the soft system is now even qualitatively different:

in this case the three statically equivalent soft-sphere volume fractions are clearly below the glass transition of the soft-sphere system. Thus, from the results in figure 7 we conclude that, although for moderately soft potentials ($\nu \gtrsim 10$) the static structural equivalence does imply dynamic equivalence to a very good approximation, for softer potentials this implication is no longer valid, particularly in the neighborhood of the glass transition.

These observations must then have implications concerning the localization of the glass transition line in the softness–concentration state space in figure 1. The assumption of static and dynamic equivalence discussed in section 3 led to the result in equation (3.9), according to which $\phi_g^{(\nu)}$ can be approximated by the product of two factors, namely, $[\sigma^{(\nu)}/\sigma^{(\mathrm{HS})}]^3$ and $\phi_g^{(\mathrm{HS})}$. The first was calculated using the blip function result in equation (3.3) and the second, $\phi_g^{(\mathrm{HS})} = 0.563$, is the result of the SCGLE theory for the glass transition volume fraction of the hard-sphere system within the Percus–Yevick/Verlet–Weis approximation for $S(k)$. If instead of the PY/VW we employ the RY approximation, for which we just determined $\phi_g^{(\mathrm{HS})} = 0.5524$, the phase diagram would be shifted to the left by a trivial factor of (0.5524/0.563). Thus, if we wish to emphasize features more fundamental than this trivial factor, rather than plotting $\phi_g^{(\nu)}$ we should instead plot the ratio $[\phi_g^{(\nu)}/\phi_g^{(\mathrm{HS})}]$ as a function of the softness parameter ν.

In figure 8 we plot in this manner the results for the glass transition line calculated using the RY static structure factor (solid circles) which is compared with the results in figure 1 (squares); in both cases we have plotted $[\phi_g^{(\nu)}/\phi_g^{(\mathrm{HS})}]$ versus ν to eliminate the discussed trivial dependence on the approximation employed. Clearly both results exhibit the same overall scenario. As expected, the numerical differences, which are negligible for large ν, become increasingly more important as the softness parameter decreases, to the extent illustrated in the figure. One consequence of these differences is that the procedure that we employed to estimate the softness parameter ν of the experimental system in section 4 would be increasingly more imprecise for much softer systems, say for $\nu \lesssim 10$.

In the simple result in equation (3.9) (and in figure 1) we used the blip function result of equation (3.3) to evaluate the factor $[\sigma^{(\nu)}/\sigma^{(\mathrm{HS})}]^3$. As explained above, we can also determine this factor using the RY approximation along with the iso-structurality condition, which provides an independent determination of the ratio $[\sigma^{(\nu)}/\sigma^{(\mathrm{HS})}]$, which is also plotted in the inset of figure 8, to be compared with its blip function counterpart. Again, both results are totally consistent between each other for large ν, but the numerical differences become important for the softest systems.

Finally, let us mention that equation (3.9), which can also be written as

$$\left[\frac{\phi_g^{(\nu)}}{\phi_g^{(\mathrm{HS})}}\right]\left[\frac{\sigma^{(\mathrm{HS})}}{\sigma^{(\nu)}}\right]^3 = 1, \tag{5.3}$$

or as $[n_g^{(\nu)}/n_g^{(\mathrm{HS})}] = 1$, is just another manner of stating that the glass transition number concentrations of a soft-sphere system, $n_g^{(\nu)}$, and of its equivalent hard-sphere system, $n_g^{(\mathrm{HS})}$, are the same. By construction, this equality is satisfied exactly by the simple result of section 3, as illustrated by the vertical dashed line in figure 1. It is not obvious, however, that the exact results will agree with this prediction, and this could only be tested by computer simulations or experimental measurements. In the meanwhile, the approximate but independent calculation of the product in the left-hand side of this equation using the RY approximation provides an indication of the degree of deviations to be expected as the softness of the system increases. The points joined with a dashed line of figure 8 represent the left-hand side of equation (5.3) calculated with the RY structure factor. The deviation of this dashed line from unity is a quantitative indication of the failure of one important assumption of the principle of static and dynamic equivalence in the limit of very soft potentials. We refer to the assumption that two soft-sphere systems that are structurally equivalent (according to the blip function or the iso-structural conditions) will also have the same number concentration. In particular, for very soft potentials at the glass transition we find that $[n_g^{(\nu)}/n_g^{(\mathrm{HS})}] > 1$. Thus, another manner to read the fact that the RY result for the left-hand side of equation (5.3) is larger than 1 for very soft potentials is that the large amount of interpenetration of the particles in this regime requires larger crowding of particles to achieve the glass transition than with more rigid potentials.

6. Conclusions

In this paper we have proposed a simple scheme for the description of the structure and dynamics of systems characterized by purely repulsive short-ranged soft potentials, modeled by the pair potential of equation (1.1), with the aim of studying the glass transition in these systems. This scheme uses the concept of static equivalence between soft- and hard-sphere systems, plus the virtually exact analytic approximation for the static structure factor of the hard-sphere system (the Percus–Yevick/Verlet–Weis approximation) to provide the static structural information needed as an input in the self-consistent generalized Langevin equation theory of colloid dynamics. This leads to simple expressions for the dynamic properties of the soft systems in terms of the corresponding properties of the hard-sphere system involving well defined rescaling rules. The most important advantage of this scheme is its conceptual and practical simplicity, particularly from the computational point of view.

This scheme allows us to quantitatively describe the effects of the softness of the potential on the dynamic arrest transition of the system. In particular, it provides a remarkably simple prediction for the glass transition line in the softness–concentration state space. This predicted glass transition line allowed us to estimate the degree of softness of the experimental system of [10] in terms of the softness parameter ν, with the result $\nu \approx 14$. In its turn, this allowed us to calculate all the dynamic properties of our model representation of this experimental system, and to establish a systematic and direct comparison of our predictions with the experimental measurements of the relaxation of concentration fluctuations in this system near and at its glass transition. Previous to this comparison, we established a

similar comparison of our theoretical predictions with the experimental results of [31] for hard-sphere dispersions. In both cases a remarkable agreement was observed without the need for adjustable parameters in approximate solutions of the relaxation equations.

The emphasis of this paper was on moderately soft-sphere systems, such as the experimental microgel particle dispersions just referred to. For these systems our simple dynamic equivalence principle is expected to be quantitatively accurate. For softer systems this accuracy must eventually break down, and a relevant question refers to the regime where this happens. Here we addressed this question by comparing the predictions of our simplified scheme, based on the dynamic equivalence principle, with the results obtained by an independent method not explicitly expected to deteriorate for softer-sphere systems. This alternative method is based on the direct calculation of the static structure factor of the soft-sphere systems, i.e. without assuming *a priori* the validity of the static equivalence principle. For this, we employed the numerical solution of the Ornstein–Zernike equation with the Rogers–Young closure. The use of this method revealed that, apart from rather trivial factors reflecting the absolute accuracy of the approximations for $S(k)$, this independent scheme leads to the same scenario of dynamic equivalence between soft- and hard-sphere systems, except for deviations that become increasingly important for increasingly softer systems. The most notorious deviation actually reveals an important feature of the glass transition in systems with very soft potentials. This refers to the fact that very soft potentials require a higher degree of crowding (i.e. larger number concentrations) to achieve the glass transition compared with the number concentration needed by a structurally equivalent hard-sphere system.

Other than this rather quantitative difference, the general conclusion is that systems with radial short-ranged soft interactions modeled by the pair potential in equation (1.1) behave in a completely analogous manner to hard spheres. This is by no means an unexpected conclusion, but we have converted this general qualitative statement into a useful quantitative theory, that will also be useful as a reference concept to contrast the behavior of other families of repulsive interactions, such as those describing the ultra-soft interactions between polymer stars and other tenuous objects. The discussion of this subject, however, is the subject of a separate communication.

Acknowledgments

This work was supported by the Consejo Nacional de Ciencia y Tecnología (CONACYT, México), grants Nos C01-47611, C02-44744 and 84076. The authors are deeply indebted to Professors J M Méndez-Alcaraz and M Chávez-Páez for generously sharing with us their Ornstein–Zernike numerical solution codes.

Appendix. Equivalence between soft-and hard-sphere systems

The equivalence principle of soft and hard spheres can be expressed by the following relation:

$$\exp(\beta u^{(\nu)}(r))g^{(\nu)}(r;n,\sigma^{(\nu)}) \approx \exp(\beta u^{(\nu')}(r))g^{(\nu')}(r;n,\sigma^{(\nu')}) \approx y^{(\mathrm{HS})}(r;n,\sigma^{(\mathrm{HS})}), \tag{A.1}$$

which expresses the approximate equality of the function $y(r)$ of two soft-sphere systems with degrees of softness ν and ν', and soft-sphere diameters $\sigma^{(\nu)}$ and $\sigma^{(\nu')}$, respectively, provided that both have the same particle number concentration n. For this equality to hold, however, the two soft-sphere diameters $\sigma^{(\nu)}$ and $\sigma^{(\nu')}$ must be related in an appropriate manner. The simplest such relationship between these two diameters is provided by the 'blip function' condition [1], which requires the volume integral of the blip function, $b^{(\nu,\nu')}(r) \equiv [\exp(-\beta u^{(\nu)}(r)) - \exp(-\beta u^{(\nu')}(r))]$, to vanish. In equation (A.1) we have included explicitly the particular case of the hard-sphere system, labeled as HS, corresponding to the limit $\nu \to \infty$.

Since there exist highly accurate analytic approximations for $y^{(\mathrm{HS})}(r;n,\sigma^{(\mathrm{HS})})$, it is convenient to approximate the radial distribution function $g^{(\nu)}(r;n,\sigma^{(\nu)})$ of the soft-sphere system with pair potential $u^{(\nu)}(r)$ by

$$g^{(\nu)}(r;n,\sigma^{(\nu)}) \approx \exp(-\beta u^{(\nu)}(r))y^{(\mathrm{HS})}(r;n,\sigma^{(\mathrm{HS})}), \tag{A.2}$$

with $\sigma^{(\mathrm{HS})}$ being the solution of

$$\int \mathrm{d}^3 r \left[\exp(-\beta u^{(\nu)}(r)) - \exp(-\beta u^{(\mathrm{HS})}(r))\right] = 0 \tag{A.3}$$

for given ν and given soft-sphere diameter $\sigma^{(\nu)}$. This allows us to approximate the static structure factor of this soft-sphere system by

$$S^{(\nu)}(k;n,\sigma^{(\nu)}) = 1 + n\int \mathrm{d}^3 r\, \mathrm{e}^{\mathrm{i}\mathbf{k}\cdot\mathbf{r}}\left[\exp(-\beta u^{(\nu)}(r))y^{(\mathrm{HS})}(r;n,\sigma^{(\mathrm{HS})}) - 1\right]. \tag{A.4}$$

Notice, however, that by adding and subtracting n times the Fourier transform of $\exp(-\beta u^{(\mathrm{HS})}(r))y^{(\mathrm{HS})}(r;n,\sigma^{(\nu')}) = g^{(\mathrm{HS})}(r;n,\sigma^{(\mathrm{HS})})$ to the rhs of this equation we may re-write it as

$$S^{(\nu)}(k;n,\sigma^{(\nu)}) = S^{(\mathrm{HS})}(k;n,\sigma^{(\mathrm{HS})}) + n\int \mathrm{d}^3 r\, \mathrm{e}^{\mathrm{i}\mathbf{k}\cdot\mathbf{r}} b^{(\nu,\infty)}(r)y^{(\mathrm{HS})}(r;n,\sigma^{(\mathrm{HS})}) \tag{A.5}$$

where $b^{(\nu,\infty)}(r) \equiv [\exp(-\beta u^{(\nu)}(r)) - \exp(-\beta u^{(\mathrm{HS})}(r))]$ is the blip function of the soft-sphere and the hard-sphere potentials. From the properties of this function, we expect that the integral in the last term of the previous equation must be negligible except for very soft potentials. Thus, the simplest approximation for the static structure factor $S^{(\nu)}(k;n,\sigma^{(\nu)})$ of the soft-sphere potential $u^{(\nu)}(r)$ is to replace it by the static structure factor of the hard-sphere potential at the same number density and diameter $\sigma^{(\mathrm{HS})}$ related to the soft-sphere diameter $\sigma^{(\nu)}$ by the condition that the integral of the blip function $b^{(\nu,\infty)}(r)$ vanishes. This results in the approximation $S^{(\nu)}(k;n,\sigma^{(\nu)}) = S^{(\mathrm{HS})}(k;n,\sigma^{(\mathrm{HS})})$, which, in terms of the scaled function $\hat{S}^{(\nu)}(\hat{k};\phi^{(\nu)})$ defined by $S^{(\nu)}(k;n,\sigma^{(\nu)}) = \hat{S}^{(\nu)}(k\sigma^{(\nu)};\phi^{(\nu)})$, reads

$$S^{(\nu)}(k;n,\sigma^{(\nu)}) = \hat{S}^{(\mathrm{HS})}(\lambda^{-1}k\sigma^{(\nu)};\lambda^{-3}\phi^{(\nu)}), \tag{A.6}$$

which is employed in section 3 to derive the scaling rules of the dynamic properties.

In practice, we approximate $\hat{S}^{(\mathrm{HS})}(y;\phi)$ by the analytic solution $\hat{S}^{(\mathrm{PY})}(y;\phi)$ of the Percus–Yevick approximation [20, 21] with the correction of Verlet and Weis [22]. The analytic result for $\hat{S}^{(\mathrm{PY})}(y;\phi)$ is given by

$$S^{(\mathrm{PY})}(y;\phi) = 1 + 12\phi\frac{G(-\mathrm{i}y;\phi) - G(\mathrm{i}y;\phi)}{\mathrm{i}y} \tag{A.7}$$

with the complex function $G(z;\phi)$ of its complex argument z defined as

$$G(z;\phi) = \frac{z\Lambda(z;\phi)}{12\phi\,[\Lambda(z;\phi) + \Sigma(z;\phi)\mathrm{e}^{z}]} \tag{A.8}$$

with

$$\Lambda(z;\phi) \equiv 12\phi((1+\phi/2)z + (1+2\phi)) \tag{A.9}$$

and

$$\Sigma(z;\phi) \equiv (1-\phi)^2 z^3 + 6\phi(1-\phi)z^2 + 18\phi^2 z - 12\phi(1+2\phi). \tag{A.10}$$

The static structure factor $\hat{S}^{(\mathrm{PY/VW})}(y;\phi)$ of the Percus–Yevick approximation with the Verlet–Weis correction is then simply defined as [22]

$$S^{(\mathrm{PY/VW})}(y;\phi) = S^{(\mathrm{PY})}(y;\phi - \phi^2/16). \tag{A.11}$$

References

[1] Hansen J P and McDonald I R 1976 *Theory of Simple Liquids* (New York: Academic)
[2] Pusey P N 1991 *Liquids, Freezing and the Glass Transition* ed J P Hansen, D Levesque and J Zinn-Justin (Amsterdam: Elsevier)
[3] Hess W and Klein R 1983 *Adv. Phys.* **32** 173
[4] Andersen H C, Weeks J D and Chandler D 1971 *Phys. Rev.* A **4** 1597
[5] Guevara-Rodríguez F de J and Medina-Noyola M 2003 *Phys. Rev.* E **68** 011405
[6] Heyes D M 1998 *J. Chem. Phys.* **107** 1963
[7] Angell C A 1995 *Science* **267** 1924
[8] Debenedetti P G and Stillinger F H 2001 *Nature* **410** 359
[9] Götze W 1991 *Liquids, Freezing and Glass Transition* ed J P Hansen, D Levesque and J Zinn-Justin (Amsterdam: North-Holland)
[10] Bartsch E *et al* 1997 *J. Chem. Phys.* **106** 3743
[11] Stiakakis E *et al* 2002 *Phys. Rev.* E **66** 051804
[12] Mladek B M *et al* 2006 *Phys. Rev. Lett.* **96** 045701
[13] Medina-Noyola M 1988 *Phys. Rev. Lett.* **60** 2705
[14] Yeomans-Reyna L and Medina-Noyola M 2001 *Phys. Rev.* E **64** 066114
[15] Yeomans-Reyna L, Acuña-Campa H, Guevara-Rodríguez F and Medina-Noyola M 2003 *Phys. Rev.* E **67** 021108
[16] Ramírez-González P, Juárez-Maldonado R, Yeomans-Reyna L, Chávez-Rojo M A, Chávez-Páez M, Vizcarra-Rendón A and Medina-Noyola M 2007 *Rev. Mex. Física* **53** 327
[17] Yeomans-Reyna L, Chávez-Rojo M A, Ramírez-González P E, Juárez-Maldonado R, Chávez-Páez M and Medina-Noyola M 2007 *Phys. Rev.* E **76** 041504
[18] Juárez-Maldonado R, Chávez-Rojo M A, Ramírez-González P E, Yeomans-Reyna L and Medina-Noyola M 2007 *Phys. Rev.* E **76** 062502
[19] Ramírez-González P, Vizcarra-Rendón A, Guevara-Rodríguez F de J and Medina-Noyola M 2008 *J. Phys.: Condens. Matter* **20** 205104
[20] Percus J K and Yevick G J 1957 *Phys. Rev.* **110** 1
[21] Wertheim M S 1963 *Phys. Rev. Lett.* **10** 321
[22] Verlet L and Weis J-J 1972 *Phys. Rev.* A **5** 939
[23] Rogers F J and Young D A 1984 *Phys. Rev.* A **30** 999
[24] Nägele G, Bergenholtz J and Dhont J K G 1999 *J. Chem. Phys.* **110** 7037
[25] Cichocki B and Hess W 1987 *Physica* A **141** 475
[26] Medina-Noyola M 1987 *Faraday Discuss. Chem. Soc.* **83** 21
[27] Medina-Noyola M and del Río-Correa J L 1987 *Physica* A **146** 483
[28] Vineyard G H 1958 *Phys. Rev.* **110** 999
[29] Arauz-Lara J L and Medina-Noyola M 1983 *Physica* A **122** 547
[30] Nägele G 1996 *Phys. Rep.* **272** 215
[31] van Megen W and Underwood S M 1994 *Phys. Rev.* E **49** 4206